



# CEPC NOTE

December 14, 2018

Draft version 0.1



## Reconstructing $K_s^0$ and $\Lambda$ in CEPC Baseline Detector

Zheng Taifan<sup>a</sup>

<sup>a</sup>*Department of Physics, Nanjing University*

### Abstract

$K_s^0$  and  $\Lambda$  are two of long lifetime decay products of  $Z$  boson which mostly decay inside tracker after flying a significant distance from the creation point. Both of them have a high probability ( $>60\%$ ) to decay into a pair of charged particles. In this paper, we use the pair of tracks left by these daughters to reconstruct the  $K_s^0$  and  $\Lambda$  in the full simulated  $Z \rightarrow q\bar{q}$  sample ( $\sqrt{s}=91.2\text{GeV}$ ) in the CEPC (Circular Electron Positron Collider) baseline detector design. The secondary vertex was reconstructed using a simple geometric method and achieved  $\epsilon \cdot P^1$  of for  $K_s^0$  and for  $\Lambda$ . For comparison, the case of ideal PID (all tracks have correct PID attached to them) was also considered.

<sup>1</sup> $\epsilon$ =efficiency,  $P$ =purity

E-mail address: zhengtf@ihep.ac.cn

© Copyright 2018 IHEP for the benefit of the CEPC Collaboration.

Reproduction of this article or parts of it is allowed as specified in the CC-BY-3.0 license.

## 1 Introduction

The CEPC is a proposed successor of the LHC, and apart from its main goal—the Higgs study, it will reach a new level of  $Z$  measurements with expected yield of up to  $10^{12}$   $Z$  bosons during its 2-year  $Z$  pole ( $\sqrt{s} = 91.2\text{GeV}$ ) run. The Figure 1 is its baseline detector concept in the CDR (conceptual design report) published in 2018. The detector is designed based on the particle flow principle, which is to reconstruct every low-level particles, and associate every hit with these particles and subsequently use them to reconstruct and analyze every physics events. The detector has tracking acceptance of  $|\cos\theta|=0.996$  and its momentum resolution can reach  $\Delta(1/p_T) \sim 2 \times 10^{-5}\text{GeV}^{-1}$ . The  $Z$  boson is important for flavor physics and within its physics study,  $K_s^0$  and  $\Lambda$  are important observables with clear signatures. Also, their well known masses can be used to assess the detector performance and provide reference for its calibration. Both of them have long life time and mostly decay inside tracker after flying a significant distance from creation points (basically IP) with majority of daughters ( $> 60\%$ ) being charged pairs. In this paper, we reconstruct these two particles using the tracks left by their charged daughter pairs in a full simulated inclusive  $Z \rightarrow q\bar{q}$  sample in the CEPC baseline detector. Due to lack of a two-track vertex finding processor and a proper PID algorithm, the vertex is found using a simple geometric method and we evaluate the effect of PID on the performance only in an ideal case, i.e. all tracks have correct PID attached to them<sup>1</sup>.

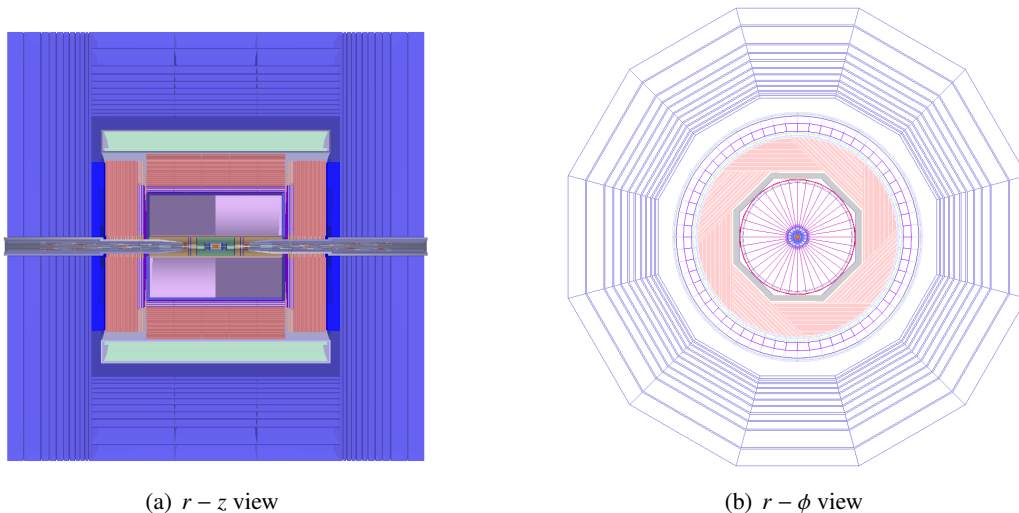


Figure 1: Baseline detector concept, from inside to outside, its basic structure consists of tracker, calorimeter, solenoid and muon detector

## 2 Sample Analysis and Reconstruction Method

Table 1 shows the basic statistics for  $K_s^0$  and  $\Lambda$  in the simulation sample. The low track reconstruction efficiency at low energy (as shown in Figure 2) is mostly due to the current track reconstruction algorithm being unable to deal properly with low momentum particles making full circles inside detector, which should be remedied in the future.

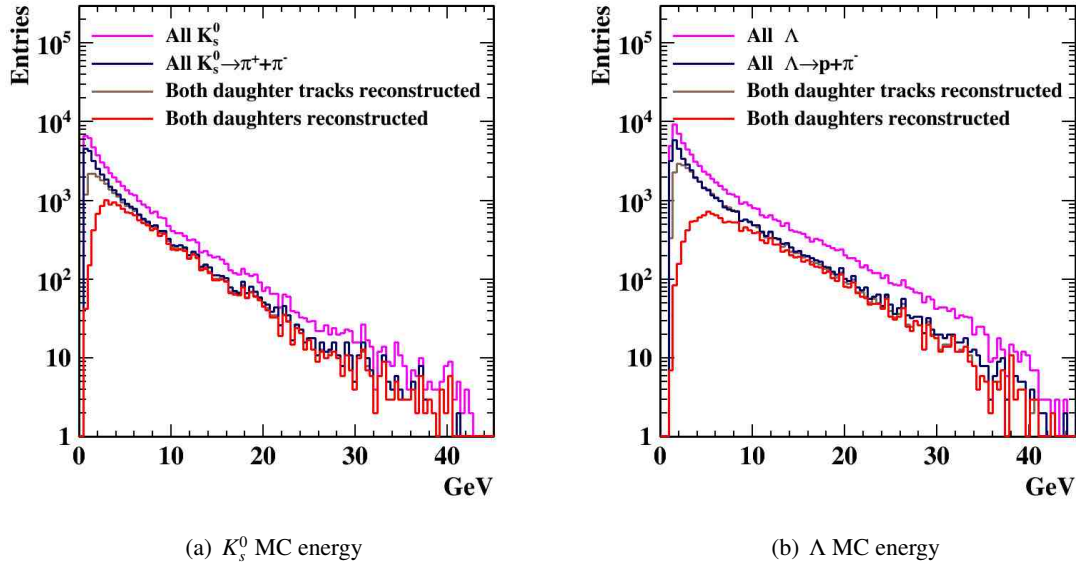
The reconstruction method for the two particles are same except some parameters, take  $K_s^0$  as an example<sup>2</sup>:

<sup>1</sup>For a given track, we can trace back all of the Monte-Carlo particles that generated its tracker hits. The ideal PID was chosen as the particle responsible for the biggest fraction of tracker hits.

<sup>2</sup>The cut parameters in the following procedure are chosen to maximize  $\epsilon \cdot P$ .

Table 1:  $K_s^0$  and  $\Lambda$  statistics for  $Z \rightarrow q\bar{q}$  simulation sample (absolute percentage)

Particle	$K_s^0$	$\Lambda$
Number of particles per event	1.0	0.14
$K_s^0 \rightarrow \pi^+\pi^-$ or $\Lambda \rightarrow p\pi^-$	67.9%	61.9%
Both daughter tracks are reconstructed	51.7%	49.9%

Figure 2: Monte-Carlo truth energy distribution of  $K_s^0$  and  $\Lambda$ 

- 36 1. Assume all of the tracks belong to either  $\pi^+$  or  $\pi^-$  depending on their sign of curvature.
- 37 2. Find the points on two track helixes where the distance is closest and it's smaller than 10mm.
- 38 3. Reconstruct 4-momentum of  $K_s^0$  using 4-momentum of daughter particles at those points and the
- 39 mass deviation from the value found in PDG is less than 10GeV.
- 40 4. The  $K_s^0$  flight path's deviation from the IP is less than 0.008 of its flight length.
- 41 Figure 3 shows how this method performs using known daughter tracks. The mass resolution is
- 42 0.26%.

### 43 3 Result and Analysis

44 With a working test result at hand, we can apply the method on the sample. The mass distributions are  
45 shown in Figure 4. Table 2 lists quantitative performances.

Table 2:  $K_s^0$  and  $\Lambda$  reconstruction performance

Particle	$K_s^0$	$\Lambda$
Mass resolution	0.29%	0.046%
$\epsilon$	76.7%	67.6%
$P$	86.0%	68.9%
$\epsilon \cdot P$	0.66	0

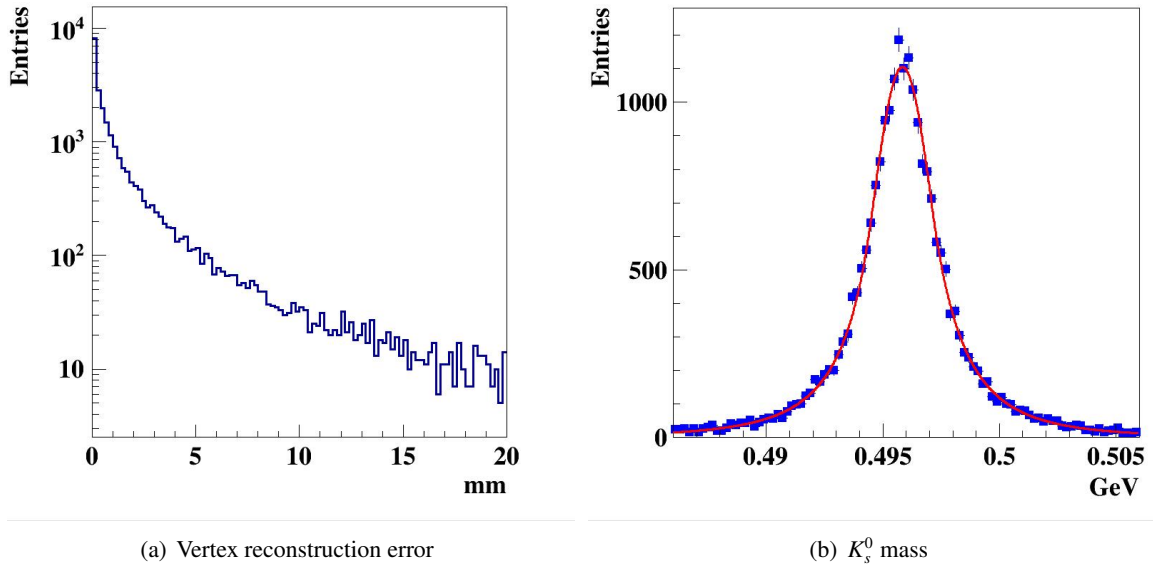


Figure 3: The performance of the method using known daughter tracks. The reconstructed vertex is the point on the track with larger  $p_T$  where the distance between the track pairs is closest.

46 Most of the backgrounds originate from random combinations (72% for  $K_s^0$  and 65% for  $\Lambda$ ). But  
 47 there are also some misidentifications because  $K_s^0$  and  $\Lambda$  because of our preassumption on track-owner-  
 48 particles.<sup>3</sup> We can improve the performance by assuming we have a perfect PID algorithm that can  
 49 identify the correct particle for every single track. The results are shown in Table 3.

Table 3:  $K_s^0$  and  $\Lambda$  reconstruction performance assuming all tracks have correct PID

Particle	$K_s^0$	$\Lambda$
Mass resolution	0.28%	0.043%
$\epsilon$	79.1%	82.3%
$P$	90.8%	93.6%
$\epsilon \cdot P$	0.72	0

## 50 4 Conclusion

51 We successfully reconstructed  $K_s^0$  and  $\Lambda$  in a inclusive  $Z \rightarrow q\bar{q}$  events in the CEPC baseline detector using  
 52 a simple geometric vertex finding and fine tuned the cut parameters for maximum  $\epsilon \cdot P$ . The reconstruc-  
 53 tion performance in an ideal PID case was also studied for comparison. The results demonstrated the  
 54 capability of the detector design and software performance but the study is also hindered by the incom-  
 55 pleteness of the software, mainly its inability to properly deal with low momentum tracks. These holes  
 56 and others such as a dedicated two-track vertex finding algorithm should be filled in the future and a  
 57 better outcome can be expected.

<sup>3</sup>One of the common ways to separate the two particles is using Armenteros plot, but it is proven to be useless in this case as we will explain in the appendix.

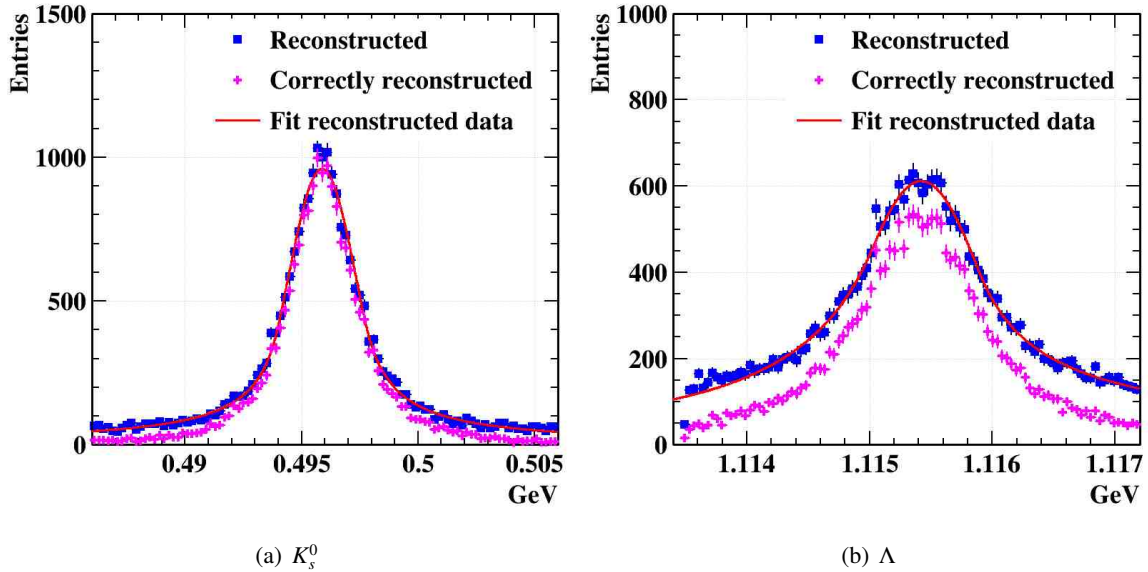


Figure 4: Reconstructed mass distribution

## 58 5 Reference

## 59 6 Appendix 1

## 60 7 Appendix 2

61 As mentioned above, the reconstruction method without resorting to a perfect PID algorithm will cause  
 62 some misidentifications between  $K_s^0$  and  $\Lambda$ . One may try to use the Armenteros plot to distinguish  
 63 them but that found out to be impossible. The Armenteros plot is the transverse momentum of positive  
 64 daughter particle ( $p_T^+$ ) versus the longitudinal momentum asymmetry ( $(p_L^+ - p_L^-)/(p_L^+ + p_L^-)$ ). Figure 7(a)  
 65 is the reconstructed  $K_s^0$  and  $\Lambda/\bar{\Lambda}$  in the Armenteros plot. The big arc in the middle is for  $K_s^0$  and the  
 66 smaller arcs at the sides are for  $\Lambda$  and  $\bar{\Lambda}$  respectively. Figure 7(b) is for all  $K_s^0$ s that are identified as  
 67  $\Lambda$ . Almost all of them are at the overlapping region of the arcs, which renders the plot useless. The  
 68 situations are same for other cases. One may also want to use the plot to separate the signal from other  
 69 backgrounds, but it too is not possible, as Figure 8 illustrates: the background is basically overlapped on  
 70 top of the signal.

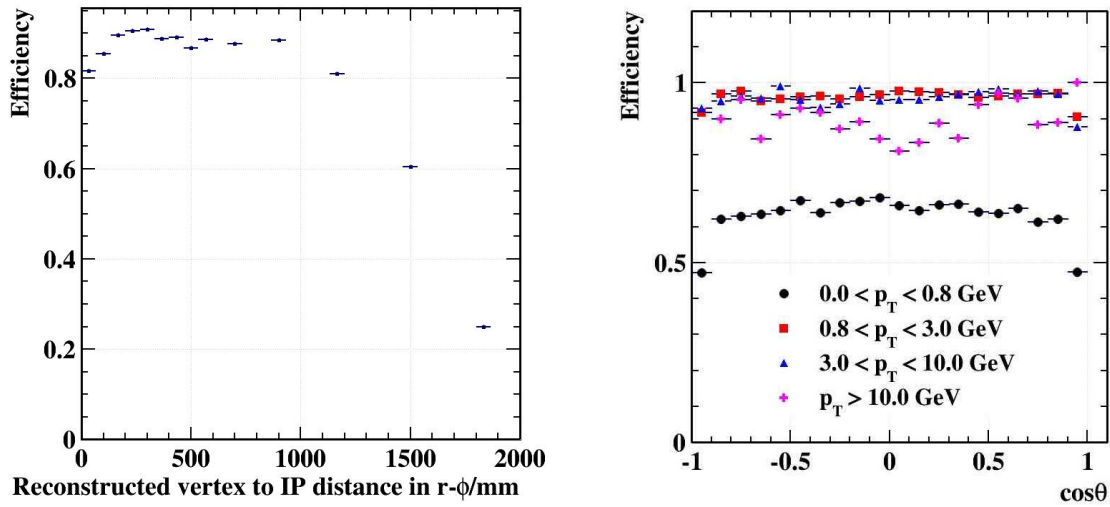


Figure 5: Vertex reconstruction efficiency for  $K_s^0 \rightarrow \pi^+\pi^-$  versus the distance from it to the IP in  $r-\phi$ , reconstruction efficiency for  $\pi^+$  from  $K_s^0 \rightarrow \pi^+\pi^-$ , which is defined as the fraction of all of the correctly selected  $\pi^+\pi^-$  pairs in comparison with all of  $\pi^+\pi^-$  tracks that have both track reconstructed. Figure 6: Polar angle and  $p_T$  dependence of track reconstruction efficiency for  $\pi^+$  from  $K_s^0 \rightarrow \pi^+\pi^-$ , which is defined as the fraction of those  $\pi^+$  that has selected  $\pi^+\pi^-$  pairs in comparison with all of  $\pi^+\pi^-$  tracks inside tracker.

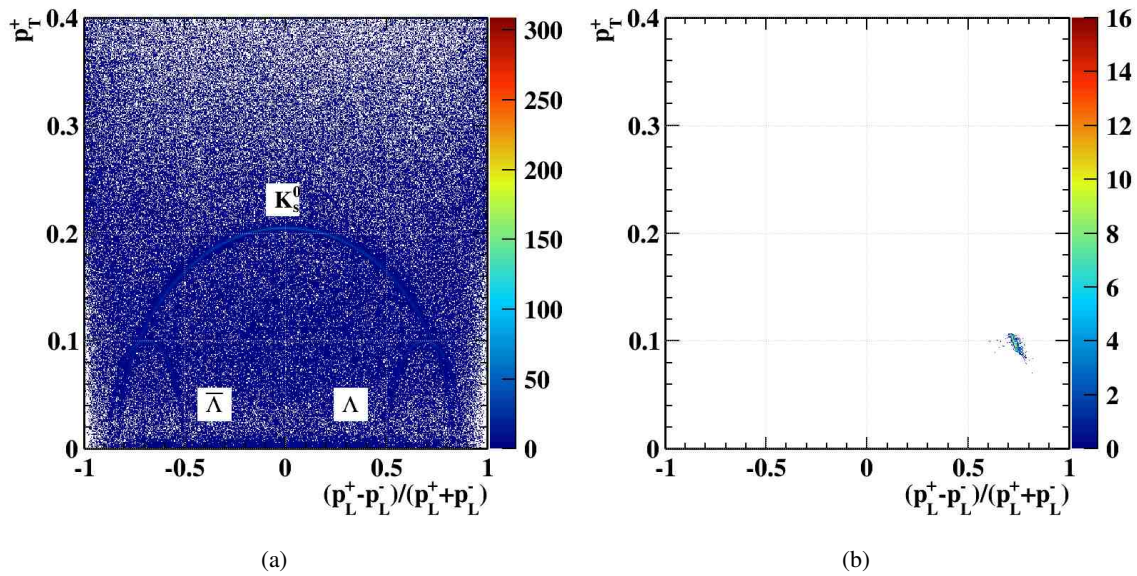


Figure 7: (a) The Armenteros plot. (b)  $K_s^0$ s identified as  $\Lambda$  in the Armenteros plot.  $p_T^+$  is the transverse momentum of the positive daughter particle with respect to the reconstructed mother's momentum.  $p_L^\pm$  is the corresponding longitudinal momentum.

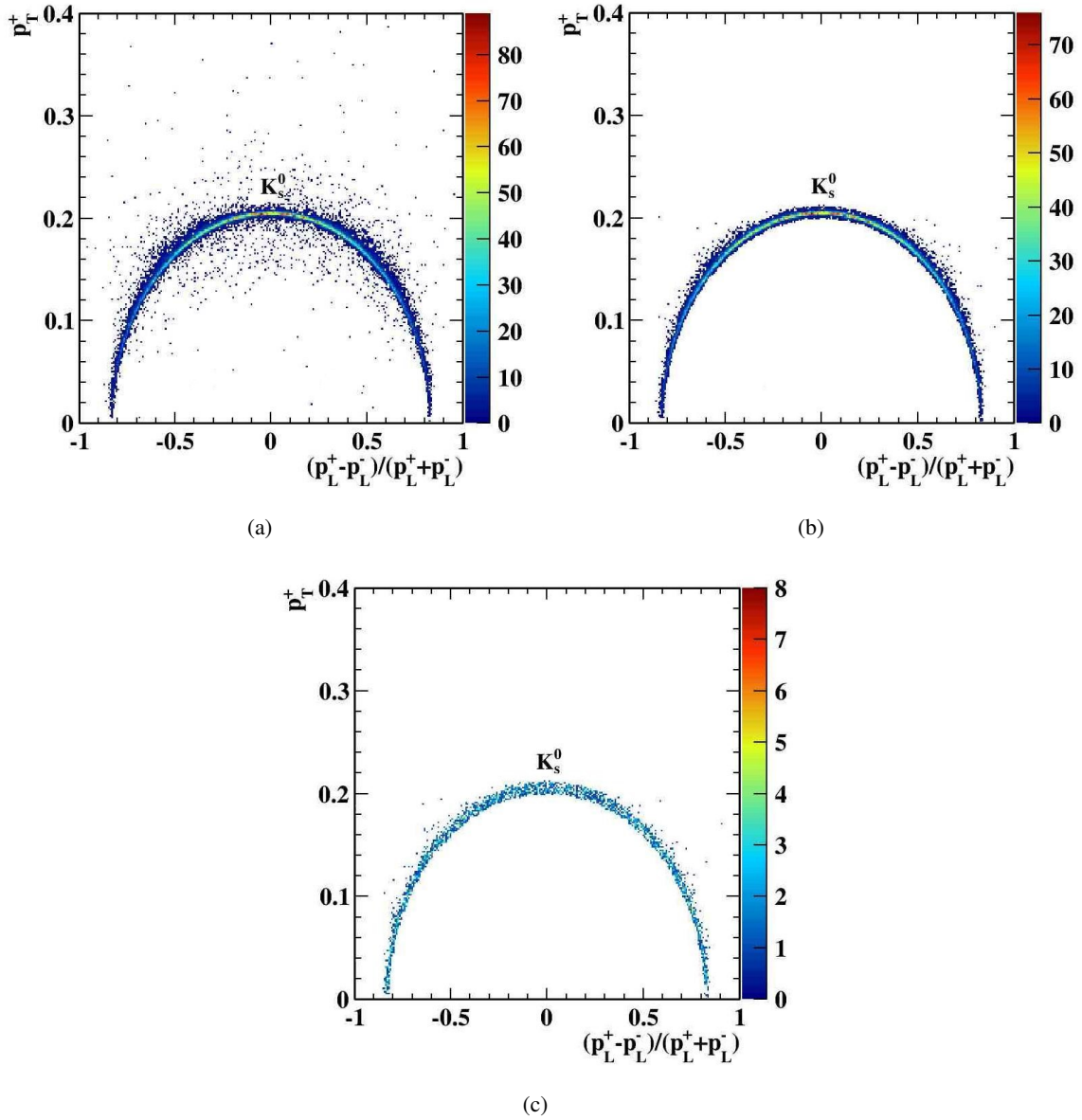


Figure 8: Armenteros plot of (a) known  $K_s^0$  daughter tracks, (b) all of the reconstructed  $K_s^0$  and (c) backgrounds in the reconstruction